Analysis for Unstable Problem of PMSM Current Control System in Overmodulation Range

Smith Lerdudomsak, Shinji Doki and Shigeru Okuma
Department of Electrical Engineering and Computer Science
Nagoya University
Nagoya, Japan
Email: smith@okuma.nuee.nagoya-u.ac.jp, doki@nagoya-u.jp, okuma@nagoya-u.jp

***Abstract*—Unstable problem of PMSM current control system in the overmodulation range of an inverter is a well known problem, however, the cause and mechanism of this problem are still not investigated well. Actually, the main reasons which are large amount of harmonic components and voltage saturation of an inverter in this range are already known. However, the effects from current controller such as PI controller gain and control period are still not considered well.**

In this paper, we focus on the effects from current controller to this unstable problem. Moreover, we also propose the easy calculation method to predict this unstable phenomena too. Compared with the simulation results, the calculation results from our proposed method match very well.

***Index Terms*—PMSM, Overmodulation range, Current control, Unstable problem**

I. Introduction

For expanding the operating range of a PMSM, there are many efforts to use an inverter in the overmodulation range. Because, compared with the conventional linear range, output voltage of an inverter in the overmodulation range can be increased as much as 127% without any increasing in dc link voltage [1].

However, a current control system of PMSM becomes unstable easily in this overmodulation range [2]-[5]. This is a well known problem of the overmodulation range, however, the reasons of unstable problem are still not analytically investigated well.

Hence, the purpose of this work is to analyze and to find the factors that make current control system of PMSM become unstable in the overmodulation range. Finally, we also propose the easy calculation method to predict the conditions that unstable problem will occur too.

II. Unstable problem in overmodulation range

Compared with the conventional linear range, there are two main differences occur in the overmodulation range [1].

1) Nonlinear relation between reference and output voltages, and also output voltage saturation (Fig.1)

2) Large amount of harmonic components in inverter output voltages, especially the 5^{th} and the 7^{th} harmonic components in phase voltages (Fig.2), or the 6^{th} harmonic component in d axis and q axis voltages

From the above differences, we can consider the model of an inverter in the overmodulation range to be equivalent to a nonlinear amplifier plus harmonics disturbance compared with a simple linear amplifier in the case of linear range as shown in Fig.3 [4].

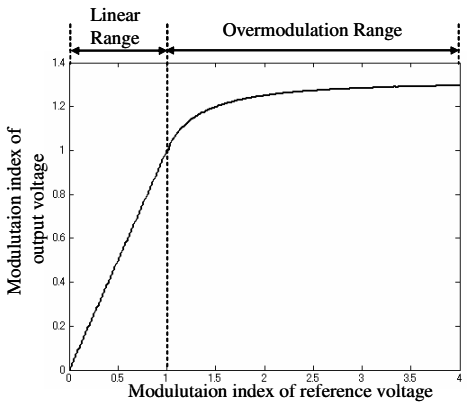

Fig. 1. The nonlinear amplitude relation between reference voltage and output voltage of an inverter

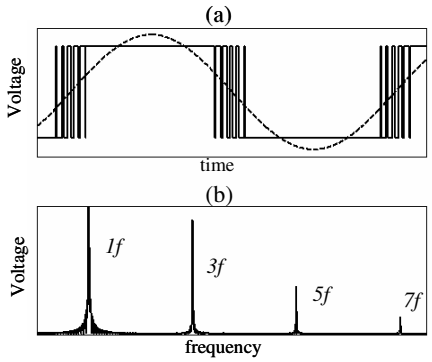

Fig. 2. (a)Wavefrom of phase voltage in overmodulation range (b)Power spectrum of voltage in overmodulation range

In a closed loop current control system of PMSM, harmonic currents that generated from inverter harmonic voltages in the overmodulation range are fed-back to closed loop system and will cause an unstable problem by the mechanism described below.

(1) PI current controllers will try to suppress these harmonic currents by generating extra disturbance suppression reference voltages to an inverter.

978-1-4244-2279-1/08/$25.00 © 2008 IEEE

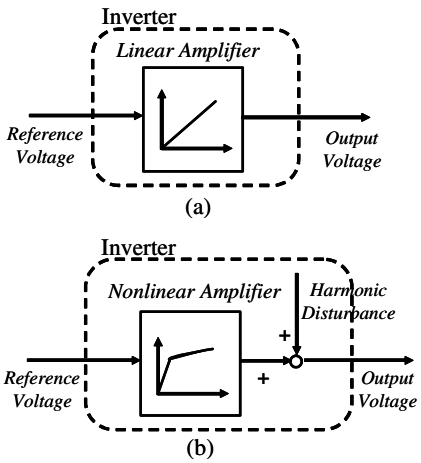

Fig. 3. Model of an inverter in (a) linear range (b) overmodulation range

(2) Becuase in the overmodulation range, inverter is already operating near the voltage saturation limit (Fig.1), an inverter will become saturated easily by these extra reference voltages.

(3) When an inverter becomes saturated, there is not enough voltage for controlling fundamental component of currents correctly, hence an unstable problem will occur.

We can say that in the overmodulation range, an unstable problem in closed loop current control system will occur or not depends on, first voltage saturation occurs or not ,and second if voltage saturation occurs, what is the voltage limiter calculation method (voltage phase control method) that be used.

In this paper we focus on the first topic that "when will the voltage saturation occur", and also find the factors in current control system that cause this saturation too. About the voltage limiter calculation method, in this paper we use the "constant d-axis voltage method" [6], however the results in this paper are also general for the other voltage limiter calculation methods too.

III. Effects from current controller

By using the conventional decoupling control method, we can consider the current control loops of d axis and q axis separately. Fig.4 shows a block diagram of current control loop, $K(s)$ is a PI current controller transfer function and $P(s)$ is a PMSM transfer function after decoupling control as shown in (1) and (2) respectively, when K_p, K_i are proportional and integral gains of PI controller and L, R are inductance and resistance of PMSM. $r(s), u(s), d(s), y(s)$ are reference current, control voltage, harmonic disturbance (generated from an inverter in the overmodulation range) and output current respectively.

$$K(s) = \frac{K_p s + K_i}{s} \quad (1)$$

$$P(s) = \frac{1}{Ls + R} \quad (2)$$

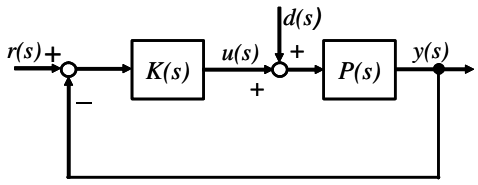

Fig. 4. Block diagram of continuous PMSM current control loop

TABLE I
PMSM PARAMETERS

pole pairs P	2
magnetic flux ϕ_m	0.104Wb
windings resistance R	0.45Ω
d-axis inductance L_d	4.15mH
q-axis inductance L_q	16.74mH

In this time, we focus on the effect from harmonic disturbance $d(s)$ to control voltage $u(s)$, and we can find the transfer function $G_{du}(s)$ that is the transfer function from $d(s)$ to $u(s)$ as shown in (3). The physical meaning of $G_{du}(s)$ is that to suppress harmonic disturbance $d(s)$, how much control voltage $u(s)$ is required.

$$G_{du}(s) = \frac{u(s)}{d(s)} = \frac{-K(s)P(s)}{1 + K(s)P(s)} = \frac{-(K_p s + K_i)}{Ls^2 + (R + K_p)s + K_i} \quad (3)$$

By using (3), we can plot the bode diagram of $G_{du}(s)$. In this time, we consider the case that the crossover frequencies of PI gain are 2,000rad/s and 10,000rad/s, and the parameters of PMSM are shown in TABLE I. Bode diagrams in these cases are shown together in Fig.5.

If we pay an attention in the magnitude of $G_{du}(s)$ in Fig.5, we can find that the larger in gain of PI controller the larger in magnitude of $G_{du}(s)$ and the easier voltage saturation will occur.

However, in a real control system, a discrete system is usually used, and we can simply model the effect of a discrete system by using the delay $e^{-T_c s}$ as shown in Fig.6, when T_c represents current control period.

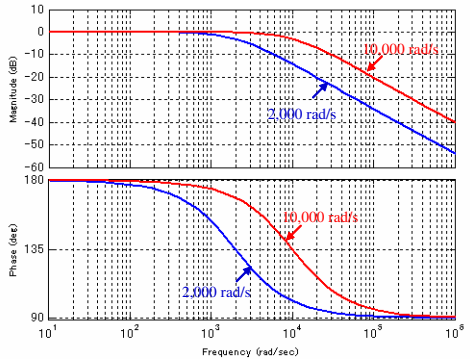

Fig. 5. Bode diagram of $G_{du}(s)$ when crossover frequencies of PI gain are 2,000 rad/s and 10,000 rad/s in continuous system

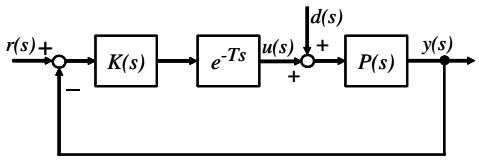

Fig. 6. Block diagram of discrete PMSM current control loop

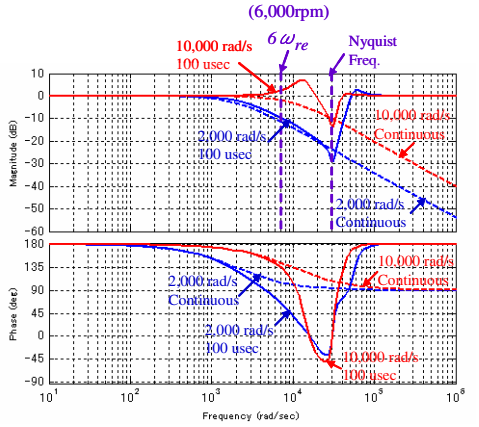

Fig. 7. Bode diagram of $G_{du}(s)$ when crossover frequencies of PI gain are 2,000 rad/s and 10,000 rad/s in continuous system and $100\mu sec$ discrete system

We can also find the transfer function $G_{du}(s)$ in this case as shown in (4). And by using Taylor approximation for delay $e^{-T_c s}$ as shown in (5), we can plot the discrete system bode diagram of $G_{du}(s)$ as shown in Fig.7, when PI gains are 2,000rad/s and 10,000rad/s and continuous and $100\mu sec$ discrete system are considered together.

$$\begin{aligned} G_{du}(s) &= \frac{u(s)}{d(s)} = \frac{-K(s)P(s)e^{-T_c s}}{1+K(s)P(s)e^{-T_c s}} \\ &= \frac{-(K_p s + K_i)e^{-T_c s}}{Ls^2 + (R + K_p e^{-T_c s})s + K_i e^{-T_c s}} \end{aligned} \quad (4)$$

$$e^{-T_c s} = 1 - T_c s + \frac{T_c^2 s^2}{2!} - \frac{T_c^3 s^3}{3!} + \frac{T_c^2 s^4}{4!} - \frac{T_c^5 s^5}{5!} \quad (5)$$

For example, if we consider the case that speed of PMSM is 6,000 rpm (the 6^{th} harmonic frequency is about 7,500 rad/s), hence from Fig.7, we can find that, the effect from discrete system makes the larger magnitude of $G_{du}(s)$, and also the easier of voltage saturation occurrence.

Next we will show the effect from PI gain by using simulation results. The parameters of PMSM are shown in TABLE I and running conditions are set for inverter to operate in the overmodulation range near the six step operation (dc link voltage is 200 V, speed is 6,000 rpm constant and reference current is 5A, 120 deg). In this time, the $100\mu sec$ control period is set to be constant, and the cases when PI gains are 2,000rad/s and 10,000rad/s are considered. The simulation results of torque and voltage amplitude in these cases are shown together in Fig.8.

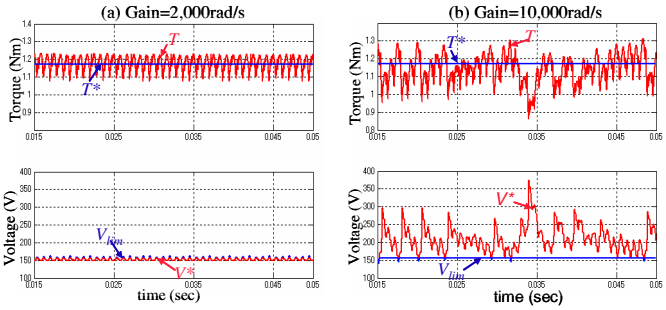

Fig. 8. Simulation results of torque and voltage amplitude when PI gains are (a) 2,000 rad/s and (b) 10,000 rad/s

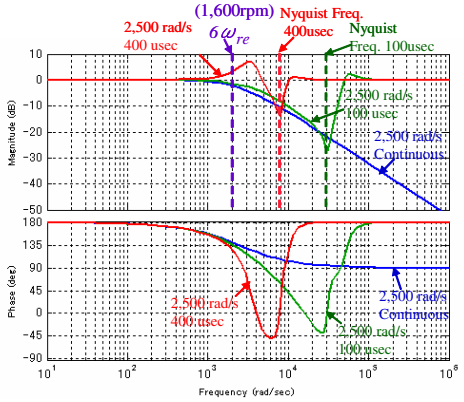

Fig. 9. Bode diagram of $G_{du}(s)$ when crossover frequencies of PI gain is 2,500 rad/s constant and control periods are 0(continuous), $100\mu sec$ and $400\mu sec$

Here, T^* and T are reference torque and real torque which are calculated from reference currents or real currents and PMSM parameters as shown in (6), V^* is an amplitude of reference voltage which can be calculated from d axis and q axis reference voltages v_d^*, v_q^* as shown in (7), and V_{lim} is limit of inverter output voltage in the overmodulation range (six step operation) which can be calculated as in (8) [1].

$$T = Pk_e i_q + (L_d - L_q) i_d i_q \quad (6)$$

$$V^* = \sqrt{v_d^* + v_q^*} \quad (7)$$

$$V_{lim} = \sqrt{\frac{3}{2}} \frac{4}{\pi} \frac{V_{dc}}{2} \quad (8)$$

From the above simulation results we can find that in the case of 2,000 rad/s, voltage saturation does not occur and torque can be stably controlled. However in the case of 10,000 rad/s, large voltage saturation occurs and torque becomes unstable. These results also conform with the bode diagram of $G_{du}(s)$ in Fig.7.

Next we will consider the effect of control period. For example, if we fix PI gain to be 2,500rad/s, and vary control period from 0(continuous), $100\mu sec$ and $400\mu sec$, the bode diagrams of $G_{du}(s)$ in these cases can be plotted together as shown in Fig.9.

In this time, if we consider the case that speed of PMSM is

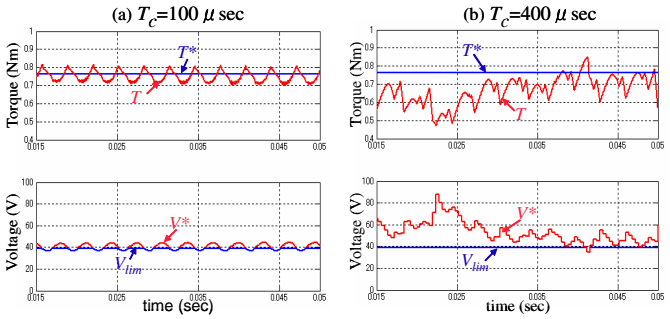

Fig. 10. Simulation results of torque and voltage amplitude when control period are (a) $100\mu sec$ and (b) $400\mu sec$

1,600 rpm (the 6^{th} harmonic frequency is about 2,000 rad/s), then from the above results, we can find that the longer in control period the larger in magnitude of $G_{du}(s)$ and the easier voltage saturation will occur.

We can also show the effect of control period by using simulation results as before. Parameters of a PMSM are shown in TABLE I and running conditions are set for inverter to operate in the overmodulation range near the six step operation (dc link voltage is 50 V, speed is 1,600 rpm constant and reference current is 3.5A, 120 deg). In this time we fix PI gain to be 2,500rad/s constant, and consider the case that control periods are $100\mu sec$ and $400\mu sec$. The simulation results are shown in Fig.10 and we can find that the results also conform with the bode diagram in Fig.9.

IV. Unstable Problem Prediction Method

Actually, an unstable problem in the overmodulation range will occur or not can be checked by experiment or computer simulation. However, this is a trial and error process and will consume so much time in system design process. Hence, in this paper we propose the more easy calculation method that can predict an unstable problem in the overmodulation range correctly. By using the proposed method, an unstable problem in the overmodulation range can be easily predicted and the results also give more insight in the unstable phenomena too.

From the above section, we can find that an unstable problem in the overmodulation range depends directly on the occurrence of voltage saturation, thus in our proposed method, we will check that how much the voltage saturation occurs and then use that result to predict an unstable problem. The calculation details are explained in step by step as below.

Step1: As the initial conditions, we assume that d axis and q axis voltages used for harmonic disturbance suppression are about 5% of decoupling voltages, thus we can calculate for d axis and q axis reference voltages v_d^*, v_q^* as shown in (9), when ω_{re} is rotational speed in rad/s (electrical degree), i_d^*, i_q^* are d and q axis reference currents respectively.

$$\begin{aligned} v_d^* &= -1.05 \times \omega_{re} L_q i_q^* \\ v_q^* &= 1.05 \times (\omega_{re} L_d i_d^* + \omega_{re} k_e) \end{aligned} \tag{9}$$

Step2: Reference voltage amplitude V^* and modulation index m_i can be calculated as shown in (10) and (11), when V_{dc} is dc link voltage. Based on the relation between reference voltage amplitude V^* and harmonic voltage amplitude as shown in Fig.11 [4], amplitudes of the 5^{th} and the 7^{th} harmonic voltages V_5, V_7 can be achieved .

$$V^* = \sqrt{v_d^{*2} + v_q^{*2}} \tag{10}$$

$$m_i = \sqrt{\frac{2}{3}} \frac{V^*}{V_{dc}/2} \tag{11}$$

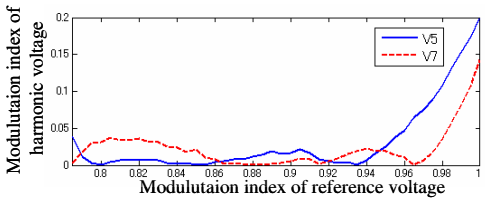

Fig. 11. Relation between modulation index of reference voltage and harmonic voltages

Step3: When the modulation index is high, the phase angles of the 5^{th} and the 7^{th} harmonic voltages can be calculated as shown in (12) [4].

$$\begin{aligned} \Phi_5 &= 5\Phi_1 = 5tan^{-1}(\frac{v_q^*}{v_d^*}) \\ \Phi_7 &= 7\Phi_1 = 7tan^{-1}(\frac{v_q^*}{v_d^*}) \end{aligned} \tag{12}$$

Step4: Based on calculated the 5^{th} and the 7^{th} harmonic voltage amplitudes and phase angles, d axis and q axis 6^{th} harmonic voltages v_{d6}, v_{q6} can be calculated as in (13) [4].

$$\begin{aligned} v_{d6} &= \sqrt{\frac{3}{2}}(V_5 cos(6\theta_{re} + \Phi_5) + V_7 cos(6\theta_{re} + \Phi_7)) \\ v_{q6} &= \sqrt{\frac{3}{2}}(-V_5 sin(6\theta_{re} + \Phi_5) + V_7 sin(6\theta_{re} + \Phi_7)) \end{aligned} \tag{13}$$

Step5: In this time we focus on the 6^{th} harmonic voltage amplitudes V_{d6}, V_{q6} that can be calculated by (14), when parameters A, B, C, D can be calculated as in (15).

$$\begin{aligned} V_{d6} &= \sqrt{\frac{3}{2}}(Asin(tan^{-1}(\frac{A}{B})) + Bcos(tan^{-1}(\frac{A}{B}))) \\ V_{q6} &= \sqrt{\frac{3}{2}}(Csin(tan^{-1}(\frac{C}{D})) + Dcos(tan^{-1}(\frac{C}{D}))) \end{aligned} \tag{14}$$

$$\begin{aligned} A &= -V_5 sin\Phi_5 - V_7 sin\Phi_7 \\ B &= V_5 cos\Phi_5 + V_7 cos\Phi_7 \\ C &= -V_5 cos\Phi_5 + V_7 cos\Phi_7 \\ D &= -V_5 sin\Phi_5 + V_7 sin\Phi_7 \end{aligned} \tag{15}$$

Step6: By using the calculation method of discrete delay as shown in (16), we can calculate for magnitude of $G_{du}(j\omega)$ of q axis current control system at frequency of 6^{th} harmonic component as shown in (17), when parameters E, F, G, H are

shown in (18). In the case of d axis current control system, K_{pq}, K_{iq}, L_q can be substituted by K_{pd}, K_{id}, L_d respectively.

$$e^{-jT_c 6\omega_{re}} = cos(T_c 6\omega_{re}) - jsin(T_c 6\omega_{re}) \tag{16}$$

$$|G_q(j6\omega_{re})| = \frac{\sqrt{(EG+FH)^2+(FG-EH)^2}}{G^2+H^2} \tag{17}$$

$$\begin{aligned} E &= K_{iq}cos(T_c 6\omega_{re}) + 6\omega_{re}K_{pq}sin(T_c 6\omega_{re}) \\ F &= -K_{iq}sin(T_c 6\omega_{re}) + 6\omega_{re}K_{pq}cos(T_c 6\omega_{re}) \\ G &= -L_q 6\omega_{re}^2 + 6\omega_{re}K_{pq}sin(T_c 6\omega_{re}) + K_{iq}cos(T_c 6\omega_{re}) \\ H &= R6\omega_{re} + 6\omega_{re}K_{pq}cos(T_c 6\omega_{re}) - K_{iq}sin(T_c 6\omega_{re}) \end{aligned} \tag{18}$$

Step7: Maximum value of voltages that used to suppress 6^{th} harmonic disturbances in d axis and q axis u_{d6}, u_{q6} can be calculated as in (19).

$$\begin{aligned} u_{d6} &= |G_d(j6\omega_{re})||V_{d6}| \\ u_{q6} &= |G_q(j6\omega_{re})||V_{q6}| \end{aligned} \tag{19}$$

Step8: Based on the calculated values of u_{d6}, u_{q6}, d axis and q axis reference voltages can be recalculated as in (20).

$$\begin{aligned} v_{d2}^* &= -(\omega_{re}L_q i_q^* + u_{d6}) \\ v_{q2}^* &= \omega_{re}L_d i_d^* + \omega_{re}k_e + u_{q6} \end{aligned} \tag{20}$$

Step9: Reference voltage amplitude is recalculated and the value "γ" can be calculated by (21).

$$\begin{aligned} V_2^* &= \sqrt{v_{d2}^{*2} + v_{q2}^{*2}} \\ \gamma &= \frac{V_2^*}{V_{lim}} = \frac{V_2^*}{\sqrt{\frac{3}{2}}\frac{4}{\pi}\frac{V_{dc}}{2}} \end{aligned} \tag{21}$$

By operating about 5 or 6 times of loop calculation from Step 2 to Step 9, the value of γ will converge. The physical meaning of "γ" is the value to show that how much reference voltage is larger than limited voltage. Of course, voltage saturation, and also unstable problem, will easily occur when γ is far above from 1.

To show the example of γ calculation results, in this time we consider the case that dc link voltage is 50 V, speed of PMSM is 1,600 rpm constant and reference current is 3.5 A. 120 deg. In this time, the gains of PI controller are varied from 1,000 rad/s to 5,000 rad/s and control periods are varied from continuous to 500 μsec discrete system. The calculation results of γ in these cases are shown together in Fig.12.

In Fig.12, the shaded area represents the operating conditions that unstable problems occur which checked by computer simulation, and of course, values of γ are much larger than 1. The simulation results in each cases are shown from Fig.13 to Fig.36. These simulation results conform with the results in Fig.12 as said before.

However in the cases of Fig.32, Fig.36 and Fig.37, the unstable characteristics are different from the others. Actually, in these conditions (very high gain and long period), an unstable problem occurs due to the discrete system closed loop

μ sec / rad/s	Cont.	100	200	300	400	500
1000	1.0268	1.0277	1.0289	1.0308	1.0344	1.0361
2000	1.0357	1.0374	1.0425	1.0477	1.3413	1.4578
3000	1.0382	1.0393	1.0443	1.3035	1.3667	1.4545
4000	1.0387	1.0408	1.0486	1.3068	1.3507	1.4018
5000	1.0424	1.0429	1.0482	1.2949	1.3361	1.3671

Fig. 12. Calculated γ values, when PI gains are 1,000 rad/s to 5,000 rad/s and control periods are 0 (continuous) to 500 μsec

poles are larger than 1, which is a normal closed loop system unstable, not by the effect from the overmodulation range. We can check that even in the linear range of an inverter, the system also becomes unstable in these conditions same as in the overmodulation range.

From the above results, we can find that the calculated γ value can be used to predict an unstable problem of closed loop current control system in the overmodulation range quite well. By using the proposed calculation method, the boundary line between stable and unstable system can be correctly predicted. However, the relation between the value of "γ" itself and the unstable degree is still not evident. One of the reasons is that, when voltage saturation occurs, the decoupling control cannot correctly operate. Hence, for more proper results, the effect from coupling terms between d axis and q axis when the voltage saturation occurs should be considered too, and this topic is one of our future works.

V. Conclusion

In this paper, the cause and the mechanism of an unstable problem in the overmodulation range of an inverter are investigated. The effects from current control system to this unstable problem which are the effects from PI controller gain and control period are analytically explained. Finally, the easy calculation method for prediction of an unstable problem are proposed and the calculation results are confirmed by the simulation results.

References

[1] A.H.Hava,R.J.Kerkman and T.A.Lipo "Carrier-Based PWM-VSI Overmodulation Strategies: Analysis, Comparison, and Design," *IEEE Trans. Power Electronics*, vol.13,no.4,Jul. 1998 pp. 674-689.

[2] A.M.Khambadkone,J.Holtz "Compensated Synchronous PI Current Controller in Overmodulation Range and Six-Step Operation of Space-Vector-Modulation-Based Vector-Controlled Drives" *IEEE Trans. Industrial Electronics*, vol.49,no.3,June. 2002 pp. 574-580.

[3] H.W.Kim,N.V Nho and M.J.Youn "Current Control of PM Synchronous Motor in Overmodulation Range," *IECON 2004* , pp. 896-901.

[4] S.Lerdudomsak, M.Kadota, S.Doki and S.Okuma "Harmonic Currents Estimation and Compensation Method for Current Control System of IPMSM in Overmodulation Range," *PCC-Nagoya 2007* , pp. 1320-1326.

[5] S.Lerdudomsak, S.Doki and S.Okuma "A Novel Current Control System for PMSM Considering Effects from Inverter in Overmodulation Range," *PEDS 2007* , pp. 794-800.

[6] S.Lerdudomsak, M.Kadota, S.Doki and S.Okuma "Novel Techniques for Fast Torque Response of IPMSM Based on Space-Vector Control Method in Voltage Saturation Region," *IECON 2007* , pp. 1015-1020.

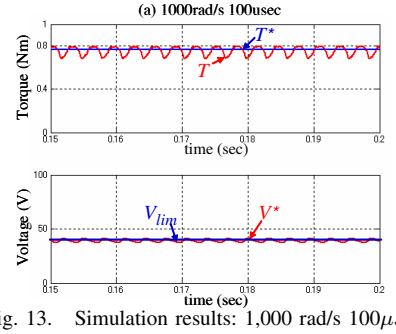

Fig. 13. Simulation results: 1,000 rad/s 100μsec

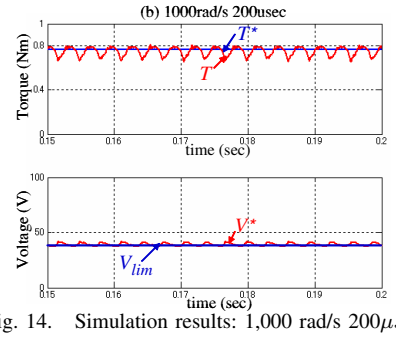

Fig. 14. Simulation results: 1,000 rad/s 200μsec

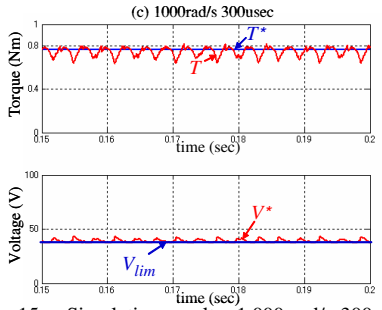

Fig. 15. Simulation results: 1,000 rad/s 300μsec

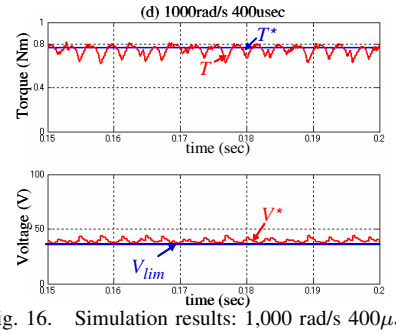

Fig. 16. Simulation results: 1,000 rad/s 400μsec

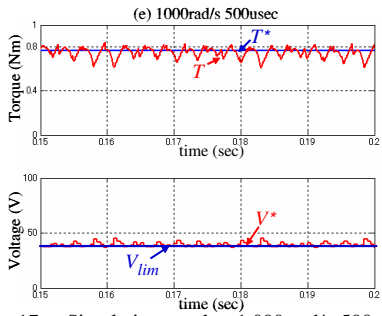

Fig. 17. Simulation results: 1,000 rad/s 500μsec

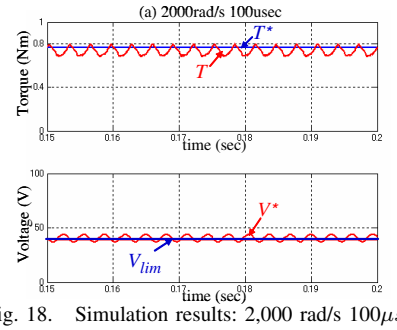

Fig. 18. Simulation results: 2,000 rad/s 100μsec

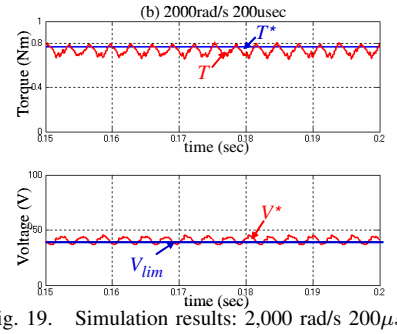

Fig. 19. Simulation results: 2,000 rad/s 200μsec

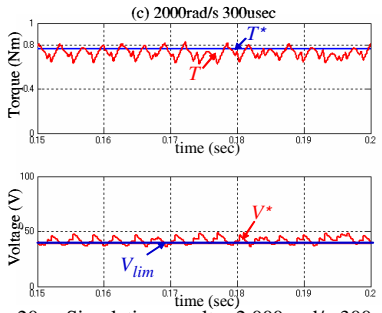

Fig. 20. Simulation results: 2,000 rad/s 300μsec

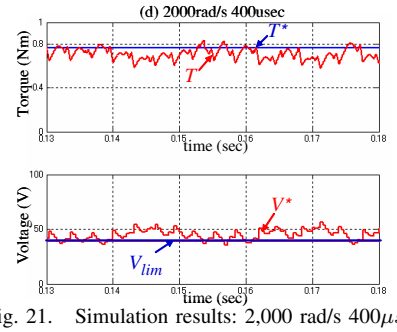

Fig. 21. Simulation results: 2,000 rad/s 400μsec

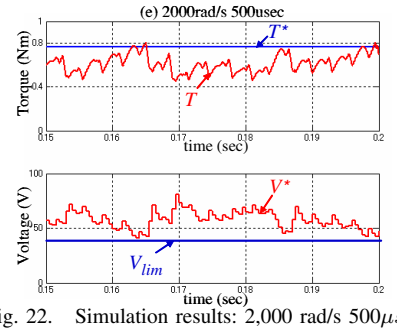

Fig. 22. Simulation results: 2,000 rad/s 500μsec

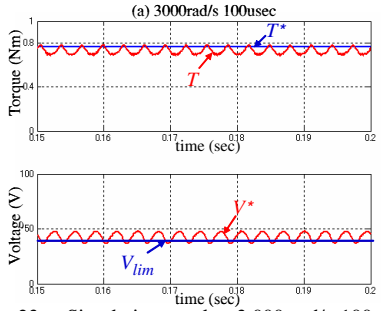

Fig. 23. Simulation results: 3,000 rad/s 100μsec

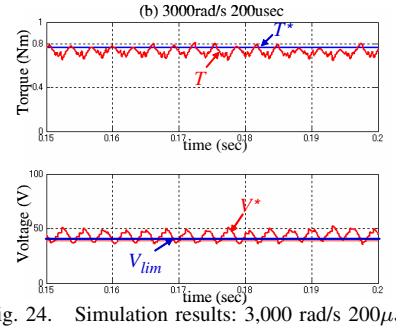

Fig. 24. Simulation results: 3,000 rad/s 200μsec

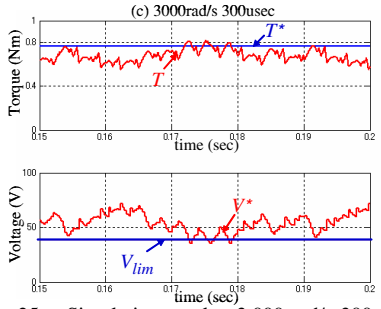

Fig. 25. Simulation results: 3,000 rad/s 300μsec

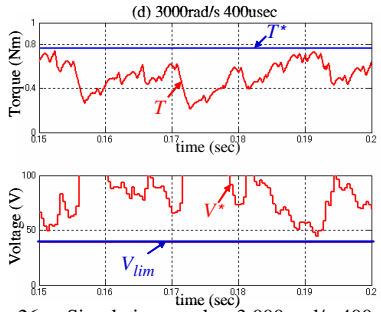

Fig. 26. Simulation results: 3,000 rad/s 400μsec

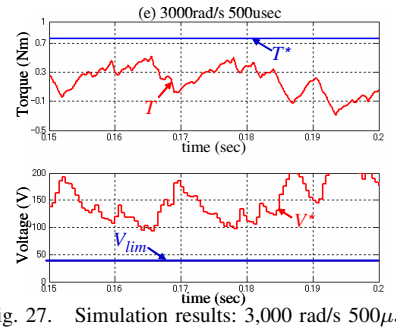

Fig. 27. Simulation results: 3,000 rad/s 500μsec

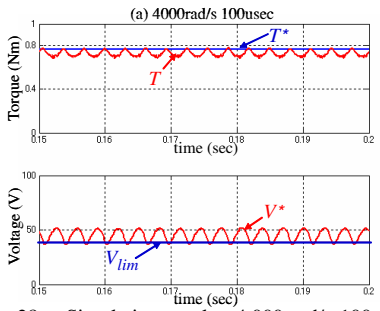

Fig. 28. Simulation results: 4,000 rad/s 100μsec

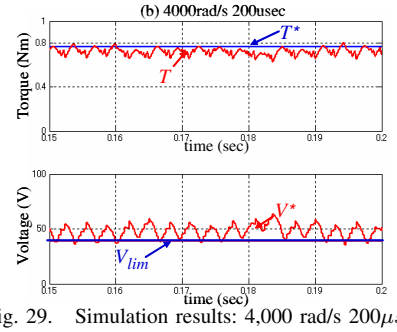

Fig. 29. Simulation results: 4,000 rad/s 200μsec

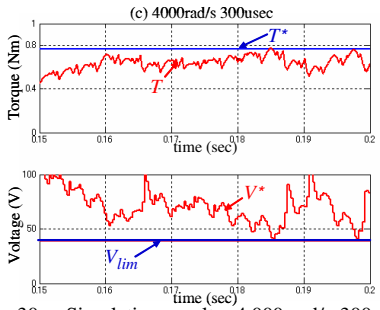

Fig. 30. Simulation results: 4,000 rad/s 300μsec

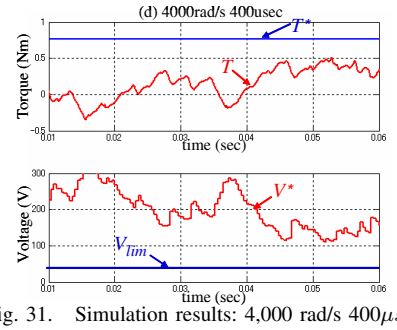

Fig. 31. Simulation results: 4,000 rad/s 400μsec

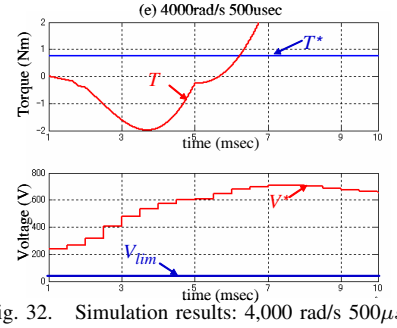

Fig. 32. Simulation results: 4,000 rad/s 500μsec

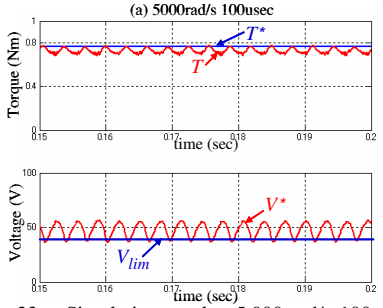

Fig. 33. Simulation results: 5,000 rad/s 100μsec

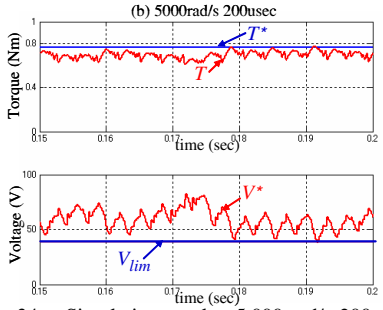

Fig. 34. Simulation results: 5,000 rad/s 200μsec

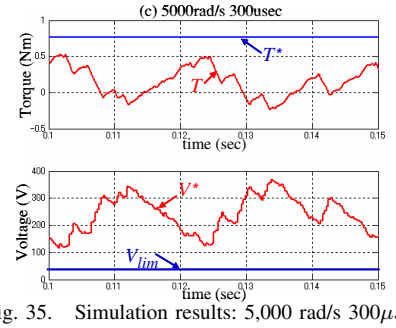

Fig. 35. Simulation results: 5,000 rad/s 300μsec

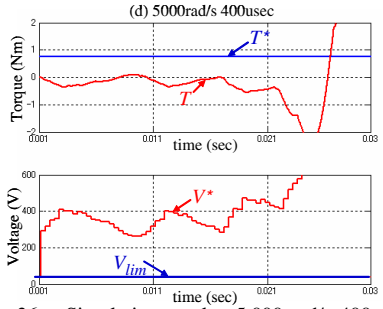

Fig. 36. Simulation results: 5,000 rad/s 400μsec

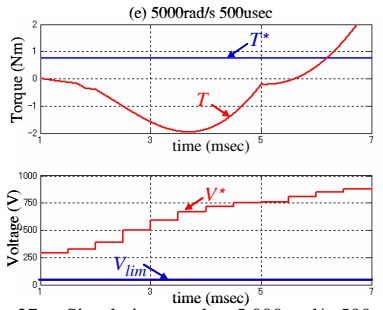

Fig. 37. Simulation results: 5,000 rad/s 500μsec